Int. J. Heat Mass Transfer. Vol. 13, pp. 439–442. Pergamon Press 1970. Printed in Great Britain

FREE CONVECTION FLOW PATTERNS AT HORIZONTAL SURFACES WITH IONIC MASS TRANSFER

A. A. WRAGG and R. P. LOOMBA

Department of Chemical Engineering, University of Manchester Institute of Science and Technology, Manchester

(*Received* 10 *January* 1969 *and in revised form* 30 *June* 1969)

NOMENCLATURE

Dimensionless groups

- Gr_h, Grashof number for heat transfer, $X^3g\beta\Delta T/\nu^2$;
- Gr_m, Grashof number for mass transfer, $X^3g\Delta\rho/\rho_i\nu^2$;
- Nu, Nusselt number, hX/k;
- Pr, Prandtl number, $C_p\mu/k$;
- Sc, Schmidt number, ν/D;
- Sh, Sherwood number, k_mX/D;
- C_p, heat capacity [cal/g.°C];
- d, surface diameter [cm];
- D, diffusion coefficient [cm^2/s];
- g, gravitational acceleration [cm/s^2];
- h, heat-transfer coefficient [cal/cm^{2}s°C];
- k_m, mass-transfer coefficient [cm/s];
- k, thermal conductivity [cal/cms°C];
- M, solution molarity;
- ΔT, temperature gradient between solid surface and bulk solution [°C];
- X, characteristic dimension of a system [cm].

Greek symbols

- β, coefficient of thermal expansion;
- ν, kinematic viscosity, μ/ρ [cm^2/s];
- μ, dynamic viscosity [g/cms];
- ρ, solution density [g/cm^3];
- $\Delta\rho$, density difference between bulk solution and interface [g/cm^3].

INTRODUCTION

A RECENT paper by Husar and Sparrow [1] has described flow visualization studies at horizontal upward facing heated surfaces for the case of spatially unrestricted convection. These authors draw attention to the lack of previous flow investigations and also to the fact that available data for such systems is limited and contradictory. The present work reports flow investigations for the analogous case of free convection mass transfer at horizontal upward facing electrodes. The study was carried out in support of recently published mass transfer work which sought to provide a fuller and more definitive correlation of data than was previously available [2]. During the course of that work interesting flow behaviour was observed visually near the electrodes and it was decided to examine these phenomena more closely in an effort to gain greater understanding of the basic transport mechanisms.

An earlier study of the problem was undertaken by Fenech and Tobias [3] which proposed an equation to describe data in turbulent flow, but as with the heat-transfer case no flow visualization work has been reported.

Whereas Husar and Sparrow used plane surfaces of various triangular, rectangular and circular geometries, we have confined our attention to plane circular electrodes but have varied diameters and also the solution bulk concentrations considerably, thus effecting a wide variation in the $Sc.Gr_m$ group. In addition our photographs have been taken from the side rather than from above, and this reveals different aspects of the convective behaviour.

CORRELATIONS FOR HEAT AND MASS TRANSFER AT HORIZONTAL SURFACES

Our previous work on this subject [2] yielded the following correlating equations for circular planes where the electrode diameter is used as the characteristic dimension.

$$Sh = 0{\cdot}64(Sc.Gr_m)^{0{\cdot}25}, 3 \times 10^4 < Sc.Gr_m < 2{\cdot}5 \times 10^7 \quad (1a)$$

and

$$Sh = 0{\cdot}16(Sc.Gr_m)^{0{\cdot}33}, 2{\cdot}5 \times 10^7 < Sc.Gr_m < 10^{12}. \quad (1b)$$

We have since revised our calculations in a manner similar to that described for other work [4], making use of more reliable diffusivity data, and the new equations are

$$Sh = 0{\cdot}72(Sc.Gr_m)^{0{\cdot}25}\ 3 \times 10^4 < Sc.Gr_m < 3 \times 10^7 \quad (2a)$$

and

$$Sh = 0{\cdot}18(Sc.Gr_m)^{0{\cdot}33}\ 3 \times 10^7 < Sc.Gr_m < 10^{12}. \quad (2b)$$

These compare very favourably with equations given by Bosworth [5] for heat transfer

$$Nu = 0{\cdot}71(Pr\,.\,Gr_h)^{0{\cdot}25}, \text{ in laminar flow} \quad (3a)$$

and

$$Nu = 0{\cdot}17(Pr\,.\,Gr_h)^{0{\cdot}33}, \text{ in turbulent flow.} \quad (3b)$$

Our new correlation is now considerably higher than that of Fishenden and Saunders [6] though they give a similar transition point of 2×10^7.

EXPERIMENTS

The mass transfer case is that in which cuprous ions are deposited at a copper surface at the limiting rate from a solution containing 1·5 M H_2SO_4 as indifferent electrolyte and various concentrations of $CuSO_4$. This is a well established technique in the measurement of liquid–solid mass transfer rates. In the main series of experiments a small Perspex cell 5 cm wide by 2·5 cm deep by 5 cm tall was used. This could be fitted with upward facing electrodes acting as cathodes of diameters 0·1, 0·2, 0·5, 1·0 and 2·0 cm and an anode of larger area was suspended just below the cell lid. The usual electrical circuit was provided to enable limiting currents to be measured. Experiments were performed with each electrode in each concentration of $CuSO_4$ solution and the steady limiting mass-transfer rates were achieved and measured in the usual way. Conditions were so varied as to provide a $Sc.Gr_m$ range from $1{\cdot}28 \times 10^4$ to $3{\cdot}25 \times 10^9$.

The flow patterns were photographed using the optical arrangement shown in Fig. 1. Light from an overhead projector, in an otherwise totally dark room, was passed through two holes, 3 and 0·5 mm, in two closely spaced parallel metal plates and then through the cell. A Linhof Super Technika 5×4 in. camera was positioned immediately behind the cell with its lens element removed so that the light passing through the cell threw the image of the cell and its contents directly on to a ground glass sheet positioned at the back of the camera. When the flow pattern was well established and clearly visible, the film compartment was substituted for the glass sheet and a number of frames exposed. The distances between the various items, arrived at by trial and error to give the best illumination and sharpest images, are shown in Fig. 1. A total of some 100 experimental conditions were photographed.

RESULTS

A selection of the resulting photographs are presented as Figs. 2–9 and the electrode diameter, solution concentration, and the value of the $Sc.Gr_m$ group is stated for each case. The boundary of the electrode surface is indicated on the lower edge of each photograph. A fuller range of photographs is presented elsewhere [8].

Figure 2 displays a very well defined straight vertical stream rising from the centre of the electrode in streamline motion. Our correlation, equation (2a) gives

$$Sh = 0{\cdot}72(Sc\,.\,Gr_m)^{0{\cdot}25}$$

to describe performance in the range $3 \times 10^4 < Sc.Gr_m < 3 \times 10^7$. The $Sc.Gr_m$ number for Fig. 2 falls within this range and confirms that we have here a purely laminar convective behaviour.

Figure 3 is of particular interest since it represents the case of a low density difference. Fenech and Tobias [3] had difficulty in obtaining reproducible and meaningful results in low concentration conditions. However, although the flow pattern is less distinct it displays a convective behaviour

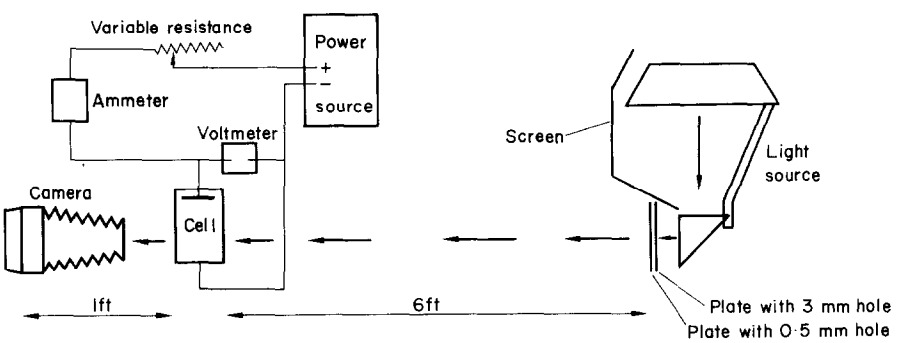

FIG. 1. Electrical and optical arrangement.

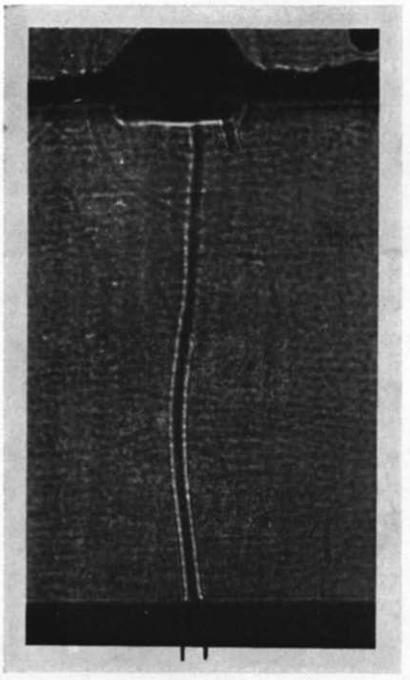

FIG. 2. $C_b = 0{\cdot}1M$, $d = 0{\cdot}2$ cm, $Sc.Gr_m = 1{\cdot}73 \times 10^6$.

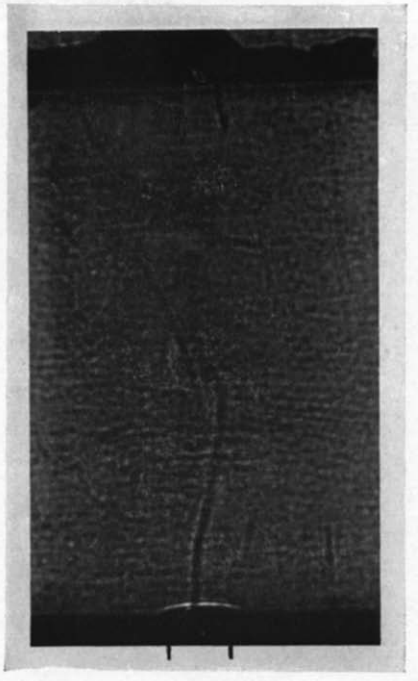

FIG. 3. $C_b = 0{\cdot}01M$, $d = 0{\cdot}5$ cm, $Sc.Gr_m = 3{\cdot}02 \times 10^6$.

FIG. 4. $C_b = 0{\cdot}2M$, $d = 0{\cdot}1$ cm, $Sc.Gr_m = 5{\cdot}1 \times 10^5$.

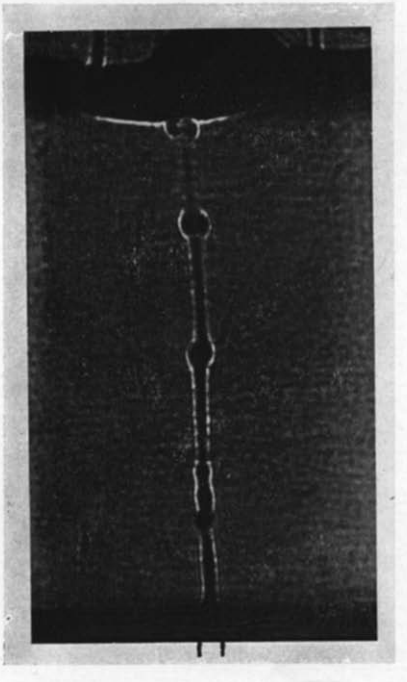

FIG. 5. $C_b = 0{\cdot}2M$, $d = 0{\cdot}2$ cm, $Sc.Gr_m = 3{\cdot}83 \times 10^6$.

[*facing page* 440]

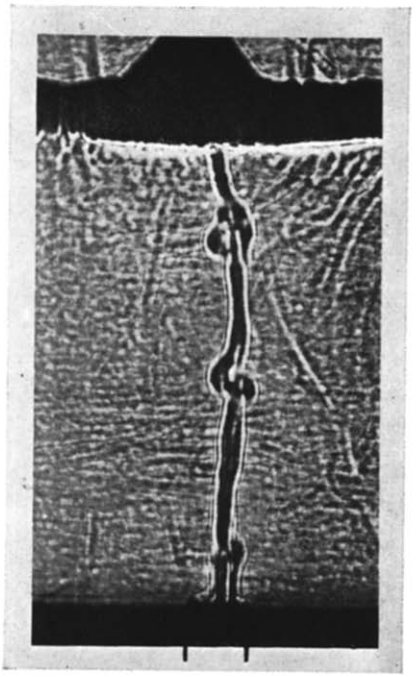

FIG. 6. $C_b = 0{\cdot}2M$, $d = 0{\cdot}5$ cm, $\mathrm{Sc.Gr}_m = 5{\cdot}9 \times 10^7$.

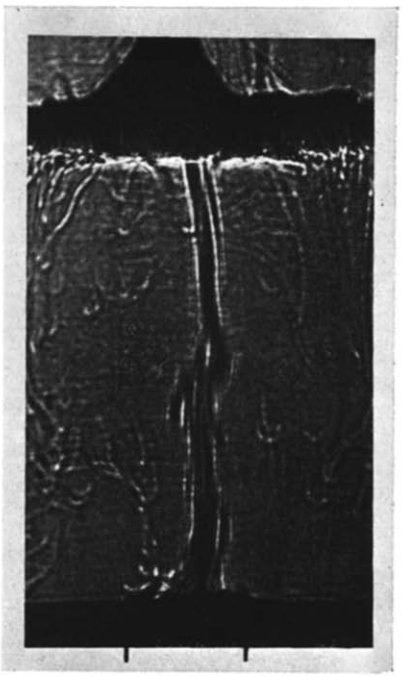

FIG. 7. $C_b = 0{\cdot}2M$, $d = 1{\cdot}0$ cm, $\mathrm{Sc.Gr}_m = 4{\cdot}44 \times 10^8$.

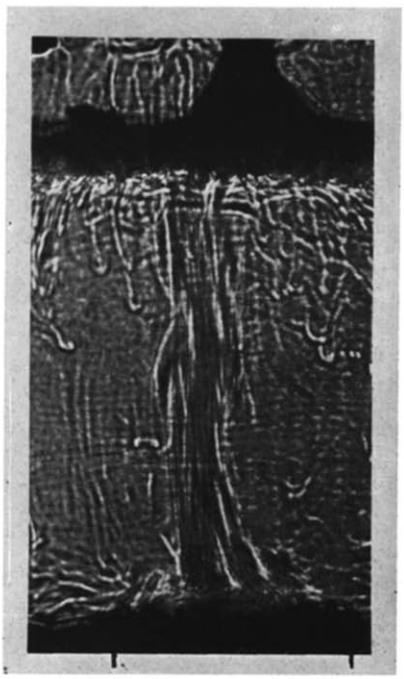

FIG. 8. $C_b = 0{\cdot}2M$, $d = 2{\cdot}0$ cm, $\mathrm{Sc.Gr}_m = 3{\cdot}26 \times 10^9$.

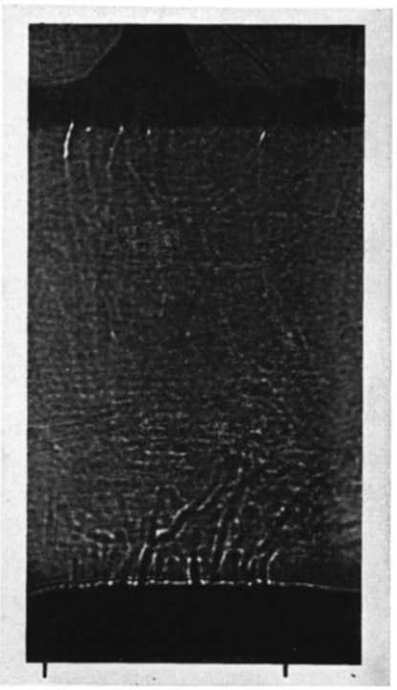

FIG. 9. $C_b = 0{\cdot}01M$, $d = 2{\cdot}0$ cm, $\mathrm{Sc.Gr}_m = 1{\cdot}74 \times 10^8$.

very similar to that of Fig. 2. One would expect therefore to find a similar and reproducible behaviour in such conditions, and our succuss in correlating this type of behaviour throughout the laminar flow regime [2] bears this out. Figure 4 again illustrates laminar behaviour with the smallest diameter electrode and the highest concentration.

Moving on to Figs. 5 and 6 we see a new type of behaviour characterized by "mushroom" formations spaced at regular intervals along the vertical convection columns. Whilst there is similarity between the behaviour shown in Fig. 5 and that of the previous photographs in that it is still largely streamline in nature, an additional mechanism is now present. The value of $Sc.Gr_m$ for Fig. 5 is $3{\cdot}83 \times 10^6$ and this probably represents the initial onset of some turbulence, pockets being carried up at fairly regular intervals in the mainly laminar stream. Flow visualization thus helps to place more precise limits on the extent of the transition region. Figure 6 illustrates another clear instance of the same kind of behaviour, though here at $Sc.Gr_m = 5{\cdot}9 \times 10^7$ the effect of turbulence is more apparent and this figure probably represents approximately the middle of the transition region.

We now turn to the higher $Sc.Gr_m$ numbers and refer to Figs. 7 and 8. The effect of anodic convection is now becoming very noticeable. Our correlation of turbulent flow data gives the equation

$$Sh = 0{\cdot}18(Sc.Gr_m)^{0{\cdot}33}$$

for the range $3 \times 10^7 < Sc.Gr_m < 10^{12}$ and these figures lie in this region. Figure 7 probably represents a condition just higher than the upper limit of the transition zone, and Fig. 8 is well into the region of fully turbulent flow and characterized by a turbulent boundary layer streaming in from the circumference and a strongly turbulent core flowing upward in the centre.

Reference to Fig. 9 reveals another important type of flow behaviour. This case lies in the transition zone just suggested but here there is no suggestion of the "mushroom" tendency. In fact the flow here is quite different from every other case, in that convection streams can be seen ascending from a number of different positions on the electrode, rather than in one central stream. The density differences are low and the width of the electrode such that we have here multi-columnar upward streamline flows, a form of cellular convection with no definite upper boundary. There are upward and downward flows at various positions across the electrode diameter.

It is thus clear that the effect of electrode diameter as well as the value of the $Sc.Gr_m$ group is an important factor in determining the convection behaviour obtaining in any specific situation. For instance, electrodes of 0·2 and 2·0 cm diameter may both have a $Sc.Gr_m$ number of $2{\cdot}5 \times 10^7$ but whereas the former might display the "mushroom" type transition behaviour, the latter might be in the region of multi-columned motion, depending on the solution concentration.

DISCUSSION

In Husar and Sparrow's heat-transfer work [1], despite a considerable variation of geometries the $Pr.Gr_h$ number has varied over a more limited range between 2×10^6 and $5{\cdot}5 \times 10^8$ which probably represents the approximate limits of the transition zone, so that characteristics of other types of behaviours are not observed. Whilst demonstrating the partition effect at corners, the heat transfer study has not revealed the changing nature of the convection which observation from the side has allowed.

It should be emphasized that the kind of behaviour observed in this work can only be expected in spatially unrestricted convection. In situations such as that commonly encountered in heat transfer where transfer occurs between two closely spaced parallel plates of considerable width, the regular cellular convective mechanism is of great importance. Newman [7] in his necessarily brief comments upon the case of electrolytic mass transfer at horizontal surfaces appears to be discussing the behaviour of a confined liquid layer since he excludes the possibility of boundary-layer flow. But he quotes the correlation of Fenech and Tobias for turbulent flow, which, despite the use of a diaphragm in the experiments parallel to the electrodes, probably reflects the spatially unrestricted case.

A further final point for comment concerns the puzzling "camelback" polarization curves which Fenech and Tobias reported for low concentration solutions with which steady mass-transfer rates were not obtained. Stoichiometrically it is clear that in 5 or 6 min the bulk concentration of reacting ion can not be so depleted as to cause such a decline in mass-transfer rates, and our flow studies indicate that steady convection obtains so that a steady mass-transfer rate would be expected. In order to clarify this situation we performed special experiments with solution concentrations down to 0·005M to investigate whether steady state mass-transfer rates could be obtained, and how quickly such conditions were established. These experiments gave thoroughly satisfactory results similar to the other laminar flow conditions, though the flow patterns were difficult to discern. The fact that Fenech and Tobias also reported erratic results with small width surfaces appears inconsistent with the very steady convection flows observed here, but was perhaps caused by their use of long narrow surfaces with a less compact flow zone and dominated by long lengths of leading edge with their associated thin boundary layers which are particularly susceptible to small disturbances.

CONCLUSION

In summary we postulate that for solid–liquid mass transfer in spatially unrestricted free convection at upward facing horizontal surfaces involving a density decrease at the transfer surface the various types of flow occur as summarized in the following scheme.

Flow type	Approximate $Sc \cdot Gr_m$ range	Comments
Laminar boundary layer and upward single column flow	$Sc \cdot Gr_m < 3 \times 10^6$	Probably occurs at only small diameter surfaces, say $d < 1$ cm
Transitional "mushroom" type flow	$3 \times 10^6 < Sc \cdot Gr_m < 2 \times 10^8$	Characteristic of small diameter electrodes and moderate and high $\Delta\rho$
Multi-columned upward flow	$Sc \cdot Gr_m > 2 \times 10^7$	Larger surfaces and small $\Delta\rho$. May lead to multi-columned turbulent ascent
Turbulent single column flow	$Sc \cdot Gr_m > 2 \times 10^8$	May partly exclude wide electrodes with low $\Delta\rho$. Here mass-transfer rate is independent of surface diameter

REFERENCES

1. R. B. HUSAR and E. M. SPARROW, Patterns of free convection flow adjacent to horizontal heated surfaces, *Int. J. Heat Mass Transfer* **11**, 1206 (1968).
2. A. A. WRAGG, Free convection mass transfer at horizontal electrodes, *Electrochim. Acta* **13**, 2159 (1968).
3. E. J. FENECH and C. W. TOBIAS, Mass transfer by free convection at horizontal electrodes, *Electrochim. Acta* **2**,
4. A. A. WRAGG and T. K. ROSS, Diffusivity and ionic mass transfer in the cupric sulphate system, *Electrochim. Acta* **13**, 2192 (1968).
5. R. C. L. BOSWORTH, *Heat Transfer Phenomena*. Wiley, N.Y. (1952).
6. M. FISHENDEN and O. A. SAUNDERS, *An Introduction to Heat Transfer*. Oxford, N.Y. (1950).
7. J. NEWMAN, Engineering design of electrochemical systems, *Ind. Engng Chem.* **60**, 12 (1968).
8. R. P. LOOMBA, Free convection mass transfer at horizontal surfaces, M.Sc. Thesis, University of Manchester (1969).